**Do model polymer therapeutics sufficiently diffuse through articular cartilage to be a viable therapeutic route?**

Alison Powell[1], Bruce Caterson[1], Clare Hughes[1], Alison Paul[2], Craig James[2], Stephen Hopkins[2], Omar Mansour[3] and Peter Griffiths[3]

[1] *School of Biosciences, Cardiff University, The Sir Martin Evans Building, Museum Avenue, Cardiff, CF10 3AX*

[2] *School of Chemistry, Cardiff University, Main Building, Park Place, CF10 3TB*

[3] *Department of Pharmaceutical, Chemical and Environmental Sciences, Faculty of Engineering and Science, University of Greenwich, Medway Campus, Central Avenue, Chatham Maritime, Kent ME4 4TB*

**Abstract**

The ability of a polymer therapeutic to access the appropriate subcellular location is crucial to its efficacy, and is defined to a large part by the many and complex cellular biological and biochemical barriers such a construct must traverse. It is shown here that model dextrin conjugates are able to pass through a cartilaginous extracellular matrix into chondrocytes, with little perturbation of the matrix structure, indicating that targeting of potential therapeutics through a cartilaginous extracellular matrix should prove possible. Rapid chondrocytic targeting of drugs which require intracellularisation for their activity, and uniform extracellular concentrations of drugs with an extracellular target, is thus enabled though polymer conjugation.

## Introduction

Articular cartilage lines the load bearing joints of the body acting to reduce friction and absorb mechanical loads. It is an aneural, avascular, hypocellular tissue, composed of a dense extracellular matrix controlled and secreted by the chondrocytes within it. The chondrocytes comprise less than 2% of the volume of mature articular cartilage with the remainder comprising a highly organised network of collagen fibrils, proteoglycans and water. The matrix macromolecules of articular cartilage give the tissue its unique structure and function. These structural macromolecules include collagens (mainly type II), proteoglycans and non-collagenous proteins. The type II collagen fibril meshwork gives the cartilage its form and tensile strength. The proteoglycans and non-collagenous proteins of articular cartilage bind to the collagen meshwork or become mechanically entrapped within it. The major proteoglycan of articular cartilage is aggrecan, which has numerous glycosaminoglycan chains attached to its core protein and forms huge multimolecular aggregates with hyaluronan and a link protein. Hydration of the glycosaminoglycan chains of aggrecan provides cartilage with its compressibility functions.

More than ten million people in the UK have long-term health problems due to arthritis or a related condition[1]. The most common arthritic diseases are osteoarthritis and rheumatoid arthritis, both of which involve erosion of the cartilage cushioning the ends of bones within the joint. Symptoms include joint-pain and stiffness, which can lead to disability. Cartilage degeneration in arthritis is due ultimately to the enzymatic degradation of the cartilage extracellular matrix. The complexity and density of the cartilage extracellular matrix results in a barrier to the passage of molecules through the matrix, however its maintenance is crucial for tissue function. In the synovial joint the articular surface is lubricated and nourished by synovial fluid, a filtrate of blood plasma containing high levels of the glycosaminoglycan hyaluronan and the proteoglycan lubricin (SZP)[2]. The relative viscosity of synovial fluid provides an additional barrier to diffusion of molecules into chondrocytes.

---

1. Arthritis and work (03.2017) http://www.arthritisresearchuk.org/policy-and-public-affairs/reports-and-resources/reports/work-report.aspx

2. Rhee, D.K., Marcelino, J., Baker, M, Gong, Y., Smits, P., Lefebvre, V., Jay, G.D., Stewart, M., Wang, H., Warman, M.L. and Carpten, J.D. (2005) The secreted glycoprotein lubricin protects cartilage surfaces and inhibits synovial cell overgrowth. The Journal of Clinical Investigation. 115: 622-631

Current therapies for arthritis mainly treat the clinical disease symptoms rather than targeting the degradative enzymes themselves. Treatments such as steroidal and non-steroidal anti-inflammatory drugs are still the mainstay of treatment[3],[4] and can have adverse side effects including high blood pressure[5],[6],[7], osteoporosis[8], cataracts[9],[10] and gastrointestinal bleeding[11]. The newly released anti-TNF drugs (Etanercept, Infliximab and Adalimumab) which block the pro-inflammatory cytokine TNF in rheumatoid and psoriatic arthritis[12],[13] are efficacious for only a small cohort of patients and are only prescribed for UK patients with severe and crippling forms of the disease as they carry the risk of serious side effects due to immuno-suppression[14].

In recent years, a number of compounds have been identified, in *in vitro* studies, that are able to inhibit the initial loss of the extracellular matrix component aggrecan, via often unknown mechanistic inhibition of the proteases ADAMTS-4 and / or -5. These compounds have notably


3. Marini, S., Fasciglione, G.F., Monteleone, G., Maiotti, M., Tarantino, U. & Coletta, M. (2003) A correlation between knee cartilage degradation observed by arthroscopy and synovial proteinases activities. Clinical Biochemistry 36: 295-304;

4. Brandt, K.D. & Slowman-Kovacs, S. (1986) Nonsteroidal anti-inflammatory drugs in treatment of osteoarthritis. Clinical Orthopaedics 213: 84-91

5. Gabriel, S.E. & Wagner, J.L. (1997) Costs and effectiveness of nonsteroidal anti-inflammatory drugs. The importance of reducing side effects. Arthritis Care Research 10:56-63

6 Hammer, F. & Stewart, P.M. (2006) Cortisol metabolism in hypertension. Best Practice and Research Clinical Endocrinology and Metabolism 20: 337-353

7 Reiche, M.L. (2005) Complications of intravitreal steroid injections. Clinical Care 76: 450-460

8 Ledford, D., Apter, A., Brenner, A.M., Rubin, K., Frieri, M. & Lukert, B. (1998) Osteoporosis in the corticosteroid treated patient with asthma. Journal of Allergy and Clinical Immunology 102: 353-363

9 Moore, P. (1997) Inhaled corticosteroids increase cataract risk. The Lancet 350: 120

10 Urban R.C. & Cotlier, E. (1986) Corticosteroid-induced cataracts. Survey of Ophthalmology 31: 102-110

11 Tringham, V.M. & Cochrane, P. (1979) Aspirin, paracetamol, diflunisal and gastrointestinal blood loss. The Lancet 320: 1409

12 Punzi, L., Podswiadek, M., Sfriso, P., Oliviero, F., Fiocco, U. & Todesco, S. (2007) Pathogenic and clinical rationale for TNF-blocking therapy in psoriatic arthritis. Autoimmunity Reviews 6(8): 524-528

13 Berthelot, J-M., Varin, S., Cormier, G., Tortellier, L., Guillot, P., Glemarec, J. & Maugars, Y. (2007) 25mg etanercept once weekly in rheumatoid arthritis and spondylarthropathy. Joint Bone Spine 74(2): 144-147

14 Maillard, H., Ornetti, P., Grimault, L., Ramon, J-F., Ducamp, S.M., Saidani, T., Tavernier, C. & Maillefert, J.F. (2005) Severe pyogenic infections in patients taking infliximab. A regional cohort study. Joint Bone Spine 72: 330-334

included the neutraceutical glucosamine[15],[16],[17] and the sulphated sugar derivative pentosan polysulphate[18],[19]. In addition, the physiological inhibitor of ADAMTS-4 and -5, TIMP-3, has been shown to ablate the initial loss of aggrecan in cytokine induced degradative mechanisms[20].

The idea that water-soluble polymers functioning as carriers of drugs through conjugation via a biodegradable spacer / linker could facilitate targeted drug release was first put forward in the mid-1970's[21]. The last two decades have seen successful clinical application of polymer conjugates to target therapeutic agents for the treatment of a range of diseases including age related macular degeneration, cancer and liver disease[22],[23],[24],[25]. These therapeutic conjugates have utilised a number of polymers as drug delivery vehicles including N-(2-hydroxypropyl)

15 Largo, R., Alvarez-Soria, M.A., Diez-Ortego, I. & Calvo, E. (2003) Glucosamine inhibits IL-1β-induced NFκB activation in human osteoarthritic chondrocytes. Osteoarthritis and Cartilage 11: 290-298

16 Maillard, H., Ornetti, P., Grimault, L., Ramon, J-F., Ducamp, S.M., Saidani, T., Tavernier, C. & Maillefert, J.F. (2005) Severe pyogenic infections in patients taking infliximab. A regional cohort study. Joint Bone Spine 72: 330-334

17 Ilic, M.Z., Martinac, B. & Handley, C.J. (2003) Effects of long-term exposure to glucosamine and mannosamine on aggrecan degradation in articulat cartilage. Osteoarthritis and Cartilage 11: 1-10

18 Smith, J.G., Hannon, R.L., Brunnberg, L., Gebski, V. & Cullis-Hill, D. (2002) A multicentre clinical study of the efficacy of sodium pentosan polysulphate and carprofen in canine osteoarthritis (osteoarthrosis).

19 Rogachefsky, R.A., Dean, D.D., Howell, D.S. & Altman, R.D. (1994) Treatment of canine osteoarthritis with sodium pentosan polysulphate and insulin-like growth factor-1. Annal of the New York Academy of Sciences 732: 392-394

20 Gendron, C., Kashiwagi, M., Hughes, C.E., Caterson, B. & Nagase, H. (2003) TIMP-3 inhibits aggrecanases-mediated glycosaminoglycan release from cartilage explants stimulated by catabolic factors. FEBS Letters 555: 431-436

21 Vasey, P.A., Kaye, S.B., Morrison, R., Twelves, C., Wilson, P., Duncan, R., Thomson, A.H., Murray, L.S., Hilditch, T.E., Murray, T., Burtles, S., Fraier, D., Frigerio, E. & Cassidy, J. (1999) Phase I Clinical and Pharmacokinetic study of PK1 [N-(2-Hydroxypropyl) methacrylamide Copolymer Doxorubicin]: First member of a new class of chemotherapeutic agents- drug-polymer conjugates. Clinical Cancer Research 5: 83-94

22 Duncan, R. (2005) Targeting and intracellular delivery of drugs. In Encyclopedia of Molecular Cell Biology and Molecular Medicine, Editor Meyers, R.A., Published by Wiley-VCH, Verlag, GmbH & Co. KGaA, Weinheim, Germany, pp163-204

23 Duncan, R. (2006) Polymer conjugates as anticancer nanomedicines. Nature Reviews Cancer 6: 688-701

24 Duncan, R., Ringsdorf, H. & Satchi-Fainaro, R. (2006) Polymer therapeutics – Polymers as Drugs, Conjugates and Gene Delivery Systems: Past, present and future opportunities. Advanced Polymer Science 192: 1-8

25 Yasukawa, T., Ogura, Y., Sakurai, E., Tabata, Y. & Kimura, H. (2005) Intraocular sustained drug delivery using implantable polymeric devices. Advanced Drug Delivery Reviews 57: 2033-2046

methacrylamide (HPMA)[26],[27], poly(ethylene glycol) (PEG)[28],[29],[30] and dextrin[31],[32]. Conjugation of drugs to polymers has allowed for specific targeting of the therapeutic activity of a drug to the diseased tissue. This results in a reduction in the dose required for efficacy of treatment and a reduction in potential toxicity of the drugs.

Expanding this modality to the treatment of arthritic joints, requires that such polymers in order to deliver their drug payload must be able to pass through a cartilaginous extracellular matrix rich in negatively charged proteoglycans, either to reach their chondrocytic targets, or to achieve even distribution throughout the cartilage extracellular matrix. In the selection of suitable targeting polymers and polymer conjugates for the treatment of arthritic disease, quantifying whether these compounds can indeed pass through the barriers presented by the synovial joint without inducing their disruption will be of vital importance. Of the potential barriers present we believe that the interactions of polymers and polymer conjugates with proteoglycans, within the cartilage extracellular matrix as well as coating its surface, will be the most influential on their movement. This study focused on investigating the interactions of polymers and polymer conjugates with the cartilage proteoglycans aggrecan and lubricin as well as synovial fluid.

---

26 Duncan, R., Vicent, M.J., Greco, F. & Nicholson, R.I. (2005) Polymer-drug conjugates: towards a novel approach for the treatment of endocrine-related cancer. Endocrine-Related Cancer 12: 189-199

27 Nan, A., Nanayakkara, N.P.D., Walker, L.A., Yardley, V., Croft, S.L. & Ghandehari, H. (2001) N-(2-hydroxypropyl)methacrylamide (HPMA) copolymers for targeted delivery of 8-aminoquinoline antileishmanial drugs. Journal of Controlled Release 77: 233-243

28 Ould-Ouali, L., Noppe, M., Langlois, X., Willems, B., Riele, P.T., Timmerman, P., Brewster, M.E., Arien, A. & Preat, V. (2005) Self-assembling PEG-ρ(CL-co-TMC) copolymers for oral delivery of poorly water soluble drugs: a case study with risperidone. Journal of Controlled Release 102: 657-668

29 Cheng, J., Teply, B.A., Sherifi, I., Sung, J., Luther, G., Gu, F.X., Levy-Nissenbaum, E., Radovic-Moreno, A.F., Langer, R. & Farokhzad, O.C. (2007) Formulation of functionalised PLGA-PEG nanoparticles for in vivo targeted drug delivery. Biomaterials 28: 869-876

30 Yu, D., Peng, P., Dharap, S.S., Wang, Y., Mehlig, M., Chandna, P., Zhao, H., Filpula, D., Yang, K., Borowski, V., Borchard, G., Zhang, Z. & Minko, T. (2005) Antitumor activity of poly(ethylene glycol)-camptothecin conjugate: The inhibition of tumor growth in vivo. Journal of Controlled Release 110: 90-102

31 Hreczuk-Hirst, D., Chicco, D., German, L. & Duncan, R. (2001) Dextrins as potential carriers for drug targeting: tailored rates of dextrin degradation by introduction of pendant group. International Journal of Pharmaceutics 230: 57-66

32 Hreczuk-Hirst, D., German, L. & Duncan, R.(2001) Dextrins as carriers for drug targeting: Reproducible succinoylation as a means to introduce pendant groups. Journal of Bioactive and Compatible Polymers 16: 353-364

## Materials & Methods

*Preparation of synovial fluid samples*

Synovial fluid samples were harvested from the metacarpo / metatarso phalangeal joints of 18 month old cows legs using a 15 gauge needle.

*Preparation of lubricin*

Following effusion of the synovial fluid from the joints of 18 month old cows legs as described above the joints were lavaged using 1.6M sodium chloride to isolate the lubricin coating the surface of the articular cartilage[33].

*Preparation of aggrecan aggregates*

Bovine articular cartilage explants were established using previous methodologies[34]. Following a 48 hour preculture explants were washed into serum free DMEM. The explants were then cultured in either (i) serum free DMEM or (ii) serum free DMEM + IL-1$\alpha$ (10ng/ml). Cultures were incubated for up to 96 hours; media and explants were harvested and finely diced prior to addition of guanidine extraction buffer (4M guanidine HCl, 50mM sodium acetate pH 5.8-6.8, 0.1M 6-amino-hexanoic acid, 5mM benzamidine HCl, 10mM ethylene diaminetetra acetic acid (EDTA) (tetrasodium salt), 1mM phenyl methyl sulphonyl fluoride (PMSF - 10ml per gram cartilage wet weight) and incubated for 48 hours at 4$^{o}$C with constant agitation. The extracted cartilage debris was removed by centrifugation at 15,000rpm for 10 minutes, and discarded. The liquid supernatant was then dialysed exhaustively against MilliQ™ water. The density of the extract was adjusted to 1.5g/ml by addition of $CaCl_2$ and aggrecan-hyaluronan aggregate purified by ultracentrifugation in a Beckman L-60 Ultracentrifuge at 37,000rpm for 70 hours at 4$^{o}$C. The extract was fractionated into 4 equal pools designated A1-A4, the lowest fraction A1 containing the purified aggrecan-hyaluronan complex and having a density >1.57g/ml.

---

33 Jones, A.R.C., Gleghorn, J.P., Hughes, C.E., Fitz, L.J., Zollner, R., Wainwright, S.D., Caterson, B., Morris, E.A., Bonassar, L.J. and Flannery, C.R. (2007) Binding and localization of recombinant lubricin to articular cartilage surfaces. Journal of Orthopaedic Research 25(3): 283-92.

34 Hughes, C.E., Caterson, B., Fosang, A.J., Roughley, P.J. and Mort, J.S. (1995) Monoclonal antibodies that specifically recognise neoepitope sequences generated by aggrecanases and matrix metalloproteinase cleavage of aggrecan: application to catabolism *in situ* and *in vitro*. The Biochemical Journal 305: 799-804

*Analysis of cellular uptake of polymer conjugates by FACS and fluorescence microscopy*

Explants were harvested and pre-cultured using previously established methods[Error! Reference source not found.] prior to incubation in the presence or absence of IL-1$\alpha$ (10ng/ml) for 96 hours[35]. Cultures were then incubated in DMEM with 50μg/ml gentamicin and 10% (v/v) heat inactivated FBS in the presence or absence of Oregon Green labelled polymers at a range of concentrations (1-10μg/ml) for a number of time points (2-24 hours). Following incubation with polymers explants were either washed in phosphate buffered saline and viewed using a confocal microscope, or digested to free the cells using Pronase (1% {w/v} in DMEM containing 50μg/ml gentamicin and 10% {v/v} heat inactivated FBS) for 30 minutes at 37$^{o}$C, followed by collagenase type II (0.4% {w/v} in DMEM containing 50μg/ml gentamicin and 10% {v/v} heat inactivated FBS) for 45 minutes at 37$^{o}$C. The isolated cells will be pelleted by centrifugation resuspended in PBS and run on a FACs Canto (BD Biosciences).

*Pulsed-Gradient Spin-Echo Nuclear Magnetic Resonance*

Measurements on the purified freeze-dried aggrecan-hyaluronan complex redispersed in $D_2O$ were conducted on a Bruker AMX360 NMR spectrometer using a stimulated echo-sequence[36]. This configuration used either a 5mm (Cryomagnet Systems, Indianapolis) or 10mm (Bruker) diffusion probe in conjunction with Bruker or Woodward gradient spectroscopy accessories.

The self-diffusion coefficient $D_s$ was extracted by fitting to equation 1 either (i) the integrals for a given peak, or (ii) the individual frequency channels present in the entire bandshape (CORE analysis);

$$A(\delta, G, \Delta) = A_o \exp[-kD_s] \qquad (1)$$

35 Arner, E.C., Hughes, C.E., Decicco, C.P., Caterson, B. and Tortorella, M.D (1998) Cytokine induced cartilage proteoglycan degradation is mediated by aggrecanases. Osteoarthritis and Cartilage. 6: 214-228

36 Davies, J.A. and Griffiths, P.C. (2003) A Phenomenological Approach to Separating the Effects of Obstruction and Binding for the Diffusion of Small Molecules in Polymer Solutions. Macromolecules: *36*, 950

where A is the signal amplitude in the absence ($A_o$) and presence of the field gradient pulses $A(\delta, G, \Delta)$) and $k = -\gamma^2 G^2 \left( \frac{30\Delta(\delta+\sigma)^2 - (10\delta^3 + 30\sigma\delta^2 + 35\delta^2\sigma + 14\sigma^3)^2}{30} \right)$

given that $\gamma$ is the magnetogyric ratio, $\Delta$ the diffusion time, σ the gradient ramp time, $\delta$ the gradient pulse length and G the gradient field strength.

*Small-angle neutron scattering*

SANS experiments were performed on the LOQ diffractometer based at the spallation source at the Rutherford Appleton Laboratory, U.K., where a *Q* range of 0.007 $Å^{-1}$ to 0.3 $Å^{-1}$ is accessible using $2 < \lambda < 10$ Å , where $Q = (4\pi/\lambda)\sin(\vartheta/2)$ $Q = \left(\frac{4\pi}{\lambda}\right) \sin\left(\frac{\theta}{2}\right)$.

Samples were contained in 1 mm pathlength, UV-spectrophotometer grade, quartz cuvettes (Hellma) and mounted in aluminium holders on top of an enclosed, computer-controlled, sample chamber. Temperature control was achieved through the use of a thermostatted circulating bath pumping fluid through the base of the sample chamber. Under these conditions a temperature stability of better than ± 0.5°C can be achieved. Experimental measuring times were approximately 40-60 min.

All scattering data were normalised for the sample transmission and the incident wavelength distribution, corrected for instrumental and sample backgrounds using a quartz cell filled with either $H_2O$ or $D_2O$ (this also removes the incoherent instrumental background arising from vacuum windows, *etc*.), and corrected for the linearity and efficiency of the detector response using the instrument specific software package. The data were put onto an absolute scale using a well-characterized partially deuterated polystyrene blend standard sample.

The intensity of the scattered radiation, *I*(*Q*), as a function of the wavevector, is given by:

$$I(Q) = NV^2(\Delta\rho)^2 P(Q) S(Q) + B_{inc} \qquad (2)$$

where $P(Q)$ describes the morphology of the scattering species, $S(Q)$ describes the spatial arrangement of the species in solution, $N$ is the number of species per unit volume, $V$ is the volume of the species, $\Delta\rho$ is the difference in the neutron scattering length density (SLD) of the scatterer and the solvent and $B_{inc}$ is the incoherent background scattering.

**Results and Discussion**

PGSE-NMR provides a convenient and non-invasive chemically selective technique for measuring translational motion, and in particular the self-, rather than mutual- diffusion coefficient. Therefore, PGSE-NMR can be used both to quantify the mobility of molecules and to assess the impact of the presence of the molecules on the extracellular matrix components themselves. The diffusion of small solutes (including water and $Na^+$) has been shown to be impeded by up to 40% by the presence of an extracellular matrix, implying that the movement of larger molecules such as polymers may be very significantly affected by the presence of a matrix[37].

A vital component in the selection of polymer-drug conjugates for the treatment of arthritic disease is the selection of either polymers able to target a drug with intracellular activity and its ability to diffuse rapidly through the extracellular matrix into the chondrocyte. Accordingly, the rate of diffusion of dextrin polymers (as model conjugates) has been quantified both in free solution and through components of the cartilaginous extracellular matrix (an aggrecan-hyaluronan aggregate gel purified by density gradient centrifugation from bovine articular cartilage), Table One. For the $M_w$ = 10k g/mol$^{-1}$ dextrin sample, the self-diffusion coefficient was slowed from $D_s = 2.7 \times 10^{-10}$ $m^2s^{-1}$ in free solution, corresponding to a hydrodynamic radius of a few nanometres, to $D_s = 2.6 \times 10^{-11}$ $m^2s^{-1}$ in the aggrecan-hyaluronan gel, (Table 1). The higher molecular weight dextrin shows a larger reduction, though the free solution retardation is consistent with the increase in molecular weight of a random coil configuration. By drawing analogies of the diffusion of such polymer in related (mucin) gels, this significant retardation is probably not a consequence of direct association of the dextrin with the aggrecan-hyaluronan aggregate, but rather steric hindrance due to the presence of the highly entangled matrix of the aggrecan-hyaluronan aggregate[38]. The non-linearity of the attenuation function clearly demonstrates the presence of more than a single diffusion rate and the CORE analysis identifies

37 Burstein, D., Gray, M.L., Hartman, A.L., Gipe, R. and Foy, B.D. (1993) Diffusion of small solutes in cartilage as measured by nuclear magnetic resonance (NMR) spectroscopy and imaging. Journal of Orthopaedic Research. 11: 465-478

38 Griffiths, P.C., Occhipinti, P., Gumbleton, M., Morris, C.J., Heenan, R.K. and King, S.M. (2010) PGSE-NMR and SANS Studies of the Interaction of Model Polymer Therapeutics with Mucin Biomacromolecules. 11: 120-125

these to be dextrin (the initial decay) and the underlying much slower (two orders of magnitude slower) diffusion of the aggrecan-hyaluronan aggregates.

As an aside, we can also comment on the effect of succinoylation – the first step in dextrin functionalisation – on the conformation of the polymer, as characterised by their self-diffusion coefficients, figure 2. The self-diffusion coefficient drops smoothly (increasing hydrodynamic size) with increasing mole percent of succinoylation, up to a value of around ~10mol%, above which the self-diffusion coefficient becomes largely constant at ~1 x $10^{-10}$ $m^2s^{-1}$, consistent with an hydrodynamic radius of around 50Å.

The (gel) structure of cartilage extract, and various derivative materials have been examined by small-angle neutron scattering (SANS) in the absence and presence of added dextrin, figures 3a&b (representative data only presented). In the case of the 18m direct cartilage extract, where the scattering from the gel itself is significant (I(Q) > 10 $cm^{-1}$ at Q < 0.01 Å) and dominates the mixture scattering (for dextrin, I(Q) < 0.5 $cm^{-1}$ at Q < 0.01 Å), addition of the two dextrin samples induced no noticeable perturbation in the scattering - and hence, structure of the direct cartilage extract gel. In the case of the IL-1 systems, and various other derivative materials (data not presented), figure 3b, the same conclusion may be drawn, but not so directly. It is obvious that the scattering does vary across the different mixed systems, but it is shown below that this is a consequence of the weaker and comparable intensities of the various components rather than one dominating contribution, as in the case of the 18m direct cartilage extract.

A number of strategies exist for interpreting SANS data. The simplest is to consider the slope of the data when plotted on a double logarithmic representation, extracting the so-called Q dependency, $I(Q) \propto Q^{-n}$, illustrating the most probable shape of the scatterer; n = 1 indicates a rod, n = 2 a flat structure, increasing all the way to n = 4 for a large, solid object. For systems like gels, one might anticipate n = 5/3 to the n = 3, reflecting a transition from a mass to volume fractal character associated with the differing length-scales present in the gel. This is indeed the case.

Alternatively, one may numerically analyse the data in terms of specific models, based on some *a priori* knowledge of the likely conformation or arrangement of molecules in solution. For

dextrin, a simple polydisperse Gaussian coil model adequately describes the data for $M_w$ = 51K g/mol$^{-1}$ dextrin sample, with $R_G$ = 80 Å (consistent with the theoretical prediction for the ratio of the radius of gyration and hydrodynamic radius, $R_G/R_H$ = 1.5).

For the gels, an appropriate treatment is the Shibayama-Geissler two-length scale model[39],[40] which treats the scattering as the additional of two components, with fraction *f*;

$$I(Q) = fI(0)_1 \frac{1}{\left(1+\left(\frac{D+1}{3}\right)Q^2a_1^2\right)^{D/2}} + (1-f)I(0)_2 exp(-Q^2a_2^2) + B \qquad (3)$$

where D is the scaling exponent and $a_2^2 \approx \frac{{R_G}^2}{3}$. The parameters describing the Shibayama-Geissler fit to these data are presented in Table Two. By and large, the fitting is most sensitive to the Lorentzian component embodied in the scaling exponent D, with a length scale ($a_1^2$) of around 100 Å, but the 18m direct cartilage extract also requires a Guinier term, with length scale slightly shorter. Most importantly, as is evident from the raw data where subtle differences are only observed at higher Q values, the parameters are largely insensitive to the addition of the dextrin *i.e.* it may be considered to be *non-perturbing*.

Having shown it is possible for dextrin to diffuse through the gel whilst having little impact on its structure, the progression of (Oregon Green fluorophore labelled) dextrin into chondrocytes was assessed. Each of the cultures was incubated in dextrin-Oregon Green at 1, 5 and 10μg/ml for 2-24 hours. Cells were released from monolayer cultures by gentle trypsinisation and by rapid pronase and collagenase digest from explant and *ex vivo* transwell grafts cultures. FACS analysis of these cell populations with 10μg/ml dextrin-Oregon Green at 2, 4, 8 and 24 hours are shown in Figure 4.

Cellular uptake of the dextrin conjugate achieved in the presence of a cartilaginous extracellular matrix in both explant cultures and in *ex vivo* transwell grafts (Figure 4B & A, respectively). In cartilage explants cellular uptake was achieved in over 90% of cells following 8 hours exposure (Figure 4B). Uptake of dextrin-Oregon Green was slower in *ex vivo* transwell grafts than in

39 Shibayama, M., Toyoichi, T., and Han, C.C. (1992) Small angle neutron scattering study on poly(N-isopropyl acrylamide) gels near their volume-phase transition temperature. J. Chem. Phys. 97(9), 6829-6841

40 Mallam, S., Horkay, F., Hecht, A.M., Rennie, A.R. and Geissler, E., (1991) Microscopic and macroscopic thermodynamic observations in swollen poly(dimethylsiloxane) networks. Macromolecules 24, 543

explants cultures with only 66% of cells containing the fluorophore following 24 hours exposure (Figure 4A). In the *ex vivo* transwell grafts the dextrin-Oregon Green was only added to the insert medium to mimic the situation *in vivo* where a therapeutic agent injected into the joint would only be able to penetrate the cartilage at the articular surface (Figure 5). This restricted access to one surface explains the apparently slower rate of uptake by chondrocytes within the *ex vivo* transwell grafts compared to chondrocytes within cartilage explants (Figures 4 A & B).

In order to determine whether dextrin-Oregon Green was able to pass right through a cartilaginous extracellular matrix it was only added to the insert medium of the *ex vivo* transwell grafts and both the insert and outer medium were analysed for its presence using fluorescence spectroscopy following a number of different incubation times (Figure 6).

The dextrin-Oregon Green was able to pass right through the extracellular matrix of the *ex vivo* transwell grafts and was detected in the outer medium of the cultures following only 2 hours of incubation with the conjugate (Figure 6). Following 24 hours incubation on the filter insert cultures over 13% of the total fluorescence present in the cultures was detected in the outer medium (Figure 6).

## Conclusions

Combined, the data presented here demonstrate that dextrin is able to successfully diffuse through a cartilaginous extracellular matrix and into the chondrocytes within, inducing little perturbation in that matrix, thus indicating the feasibility of drug delivery using polymer conjugates for the treatment of arthritis.

## Acknowledgements

EPSRC are thanked for the provision of an EPSRC Platform Grant (EP/C013220/1) ”Bioresponsive polymer therapeutics; synthesis and characterisation of novel nanomedicines”, STFC for access to SANS facilities and both Cardiff University and University of Greenwich for financial support.

**Tables**

| Sample | Free solution | Aggrecan-hyaluronan | Ratio |
|---|---|---|---|
| $M_w$ = 10K g/mol$^{-1}$ | 2.7 x 10$^{-10}$ m$^2$s$^{-1}$ | 2.6 x 10$^{-11}$ m$^2$s$^{-1}$ | 10 |
| $M_w$ = 51K g/mol$^{-1}$ | 1.0 x 10$^{-10}$ m$^2$s$^{-1}$ | 5.0 x 10$^{-12}$ m$^2$s$^{-1}$ | 20 |

***Table 1**; Self-diffusion coefficients in free solution (concentration 1wt%) and aggrecan-hyaluronan gels measured by PGSE-NMR, and the retardation ratio from free solution to gel.*

| Sample | Guinier scale | Lorentzian scale | Radius of gyration / Å | Fractal dimension | Correlation length / Å |
|---|---|---|---|---|---|
| 18m | 0.2 | 18 | 85 (+/- 3) | 2.2 (+/- 0.1) | 235 (+/- 30) |
| 18m *plus* dextrin 10K g mol$^{-1}$ | n/a | 18 | n/a | 2.3 | 140 |
| 18m *plus* dextrin 51K g mol$^{-1}$ | n/a | 14 | n/a | 2.3 | 135 |
| IL-1 | n/a | 0.2 | n/a | 2.2 | 105 |
| IL-1 *plus* dextrin 51K g mol$^{-1}$ | 0.3 | 1.1 | 55 | 2.2 | 90 |

***Table 2:** Parameters derived from an analysis of the scattering data in terms of the Shibayama-Geissler two-length scale model.*

**Figures**

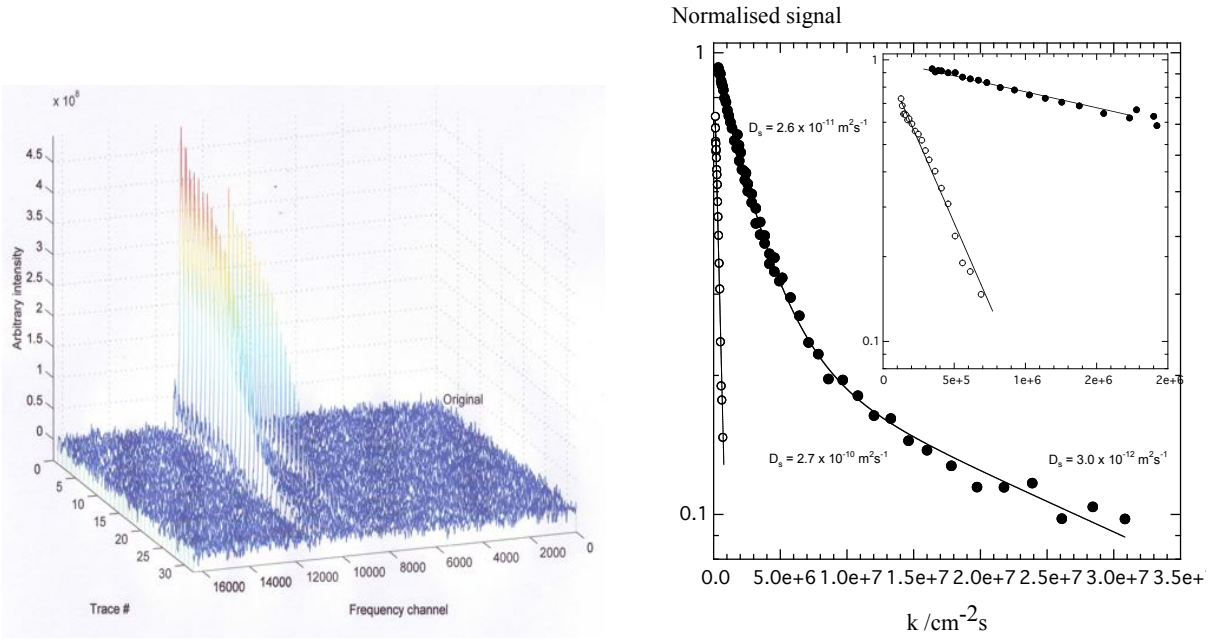


***Figure 1.*** *Experimental two-dimensional PGSE NMR dataset (left) and analysis of peak integrals used to extract the rates of diffusion (right) for $M_w$ = 10k g/mol$^{-1}$ dextrin in free solution and in an aggrecan-hyluronan gel, the open symbols correspond to the attenuation function for the peak at ~3ppm in the spectrum from 10mg/ml (1wt%) dextrin in solution i.e. the raw data presented above. The filled symbols correspond to <u>two</u> superimposed datasets, necessary to span the wide dynamics range present in these systems, again for the 3ppm peak, arising from the spectrum of 10mg/ml (1wt%) dextrin in an aggrecan-hyaluronan gel (20mg/ml GAG).*

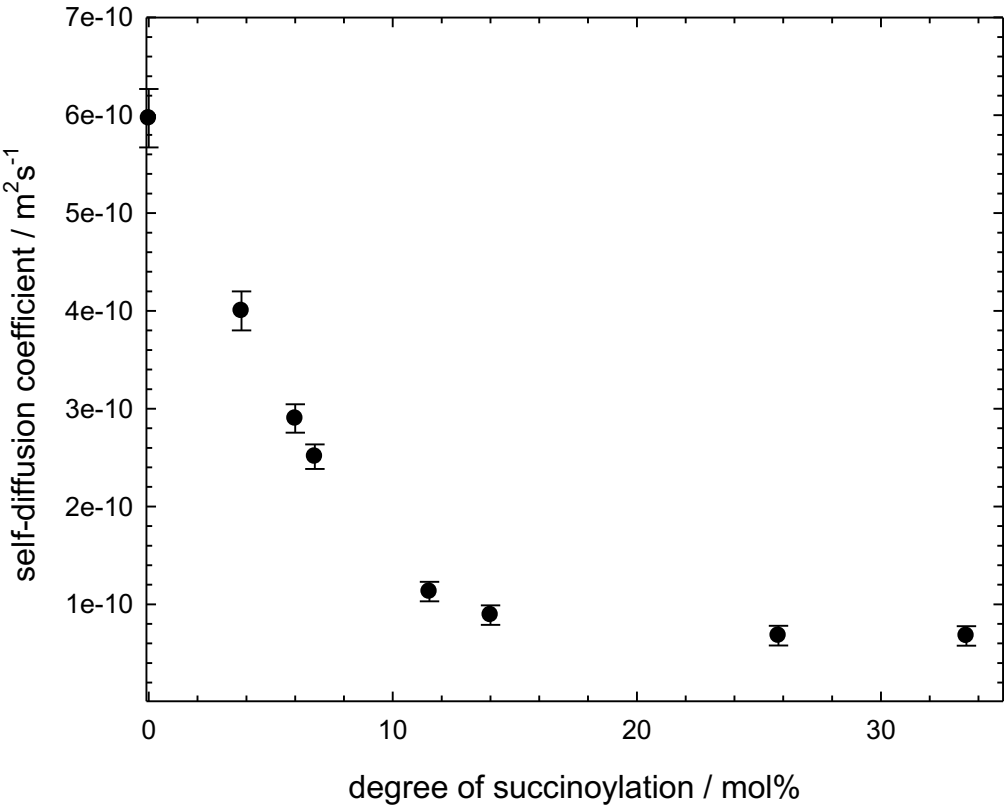


***Figure Two**; Self-diffusion coefficients in free solution as a function of degree of succinoylation measured by PGSE-NMR for dextrin $M_w$ = 51K g/mol$^{-1}$ at 1wt% polymer.*

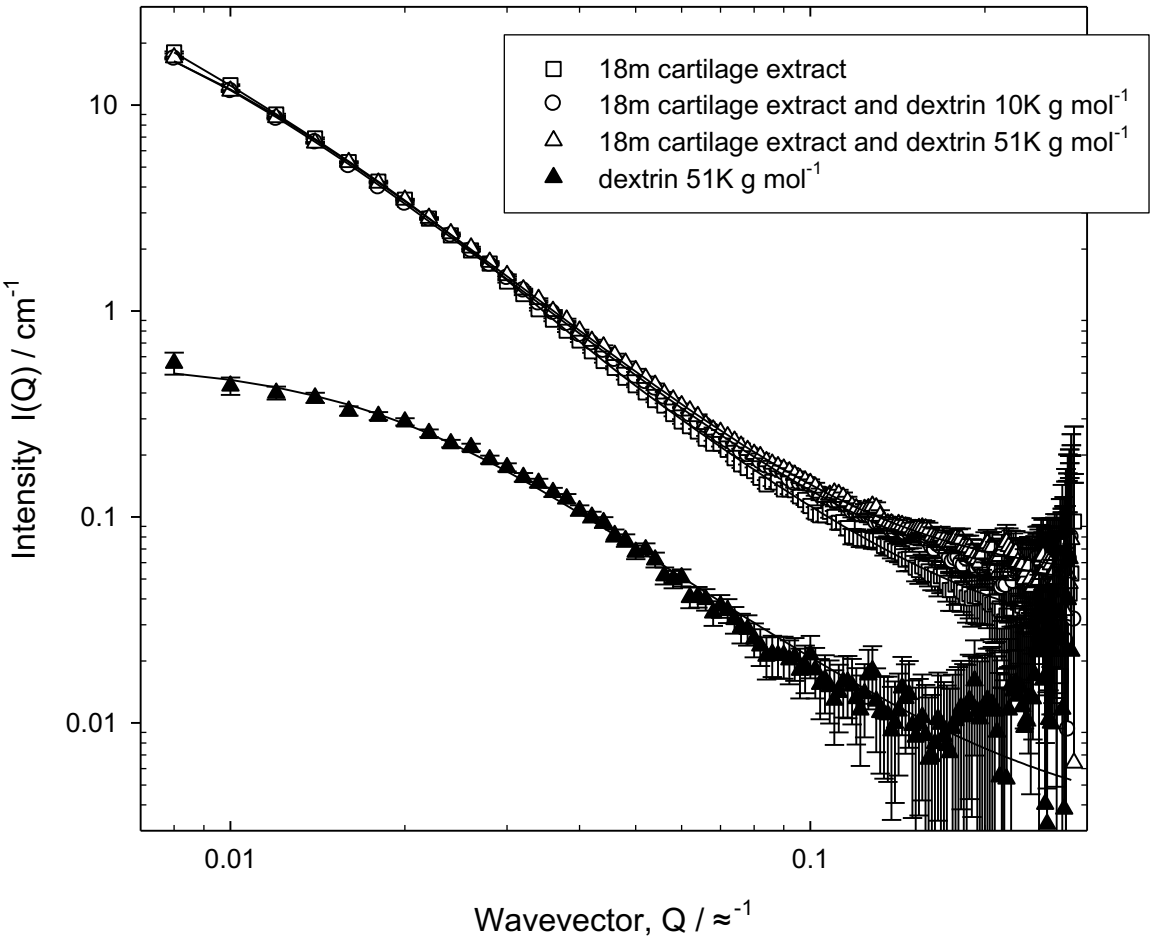


***Figure 3a.*** *Small-angle neutron scattering from 1mm thick ($H_2O$) aqueous solutions of direct cartilage extract from 18 month old knee joints in the absence of dextrin, and in the presence of 1wt% dextrin, $M_w$ = 10k g/mol$^{-1}$ and $M_w$ = 51k g/mol$^{-1}$. The lines of best fit have been derived from the analysis using the Beaucage model as described in the text. Also shown for comparison is the scattering from 1wt% $M_w$ = 51k g/mol$^{-1}$ dextrin (in $D_2O$). The lines of best fit for this dextrin sample has been derived from a simple Gaussian coil model, $R_G$ = 80 (± 3) Å.*

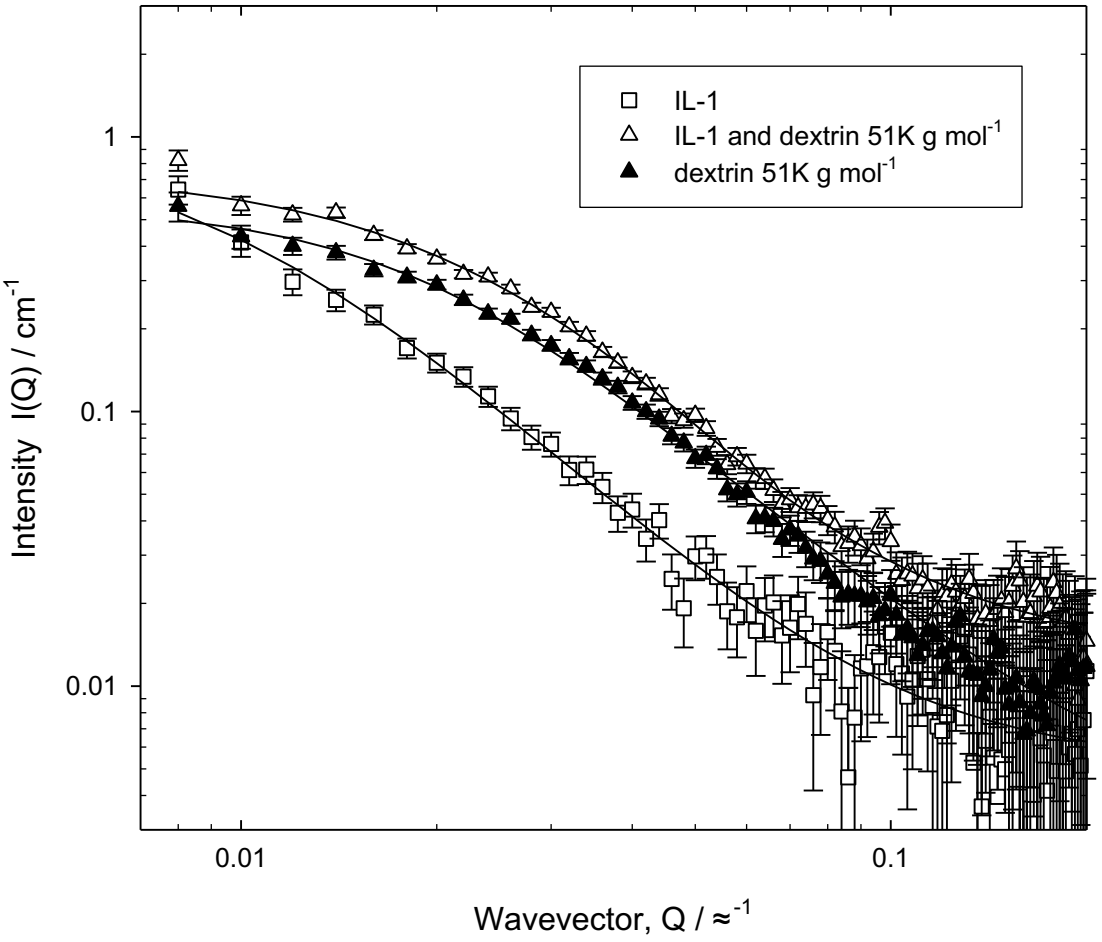


***Figure 3b.*** *Small-angle neutron scattering from 2mm thick ($D_2O$) reconstituted aqueous solutions of IL-1 in the absence of dextrin and in the presence of 1wt% dextrin $M_w$ = 51k g/mol$^{-1}$. The lines of best fit have been derived from the analysis using the gel plus coil model as described in the text. Also shown for comparison is the scattering from the dextrin solution.*

**A.** Transwell Filter Grafts **B.** Cartilage Explants

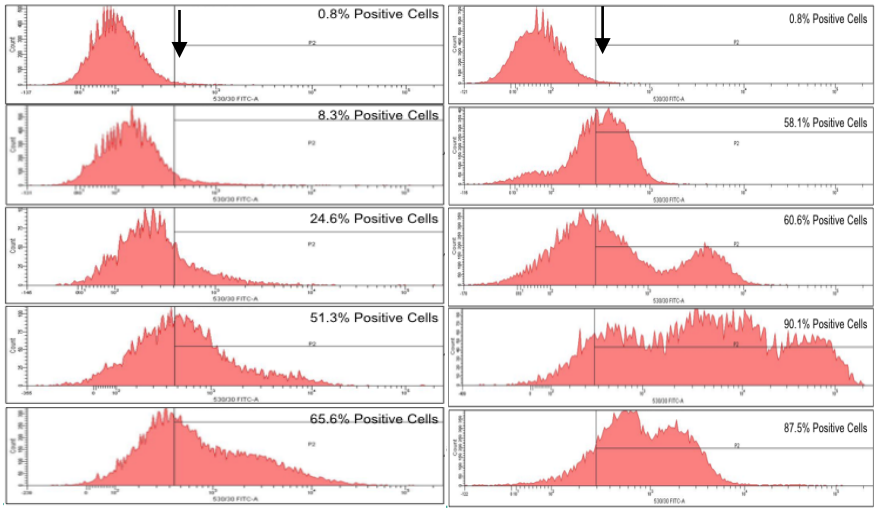


***Figure 4;*** *FACS analysis of dextrin-Oregon Green uptake with time in: (A) chondrocytes isolated from ex vivo transwell grafts following exposure to dextrin-Oregon Green and (B) chondrocytes isolated from articular cartilage explants cultures following exposure to dextrin-Oregon Green.*

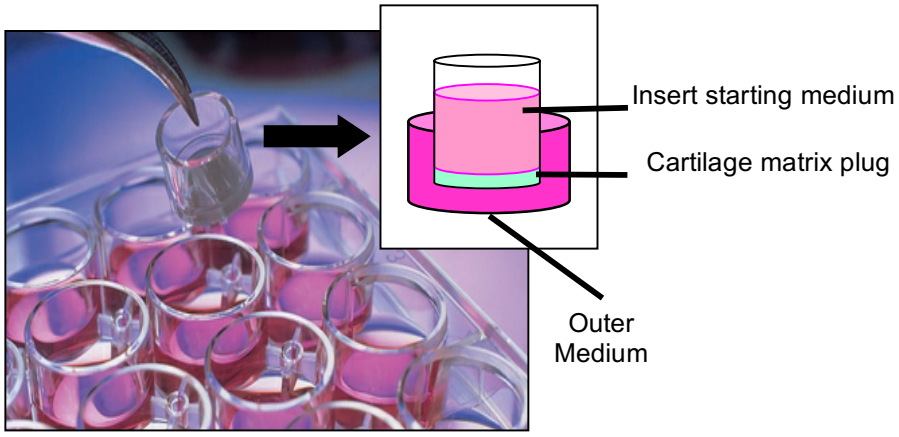


***Figure 5:*** *Picture of ex vivo transwell grafts and diagrammatic representation of the structure of the cultures (insert)*

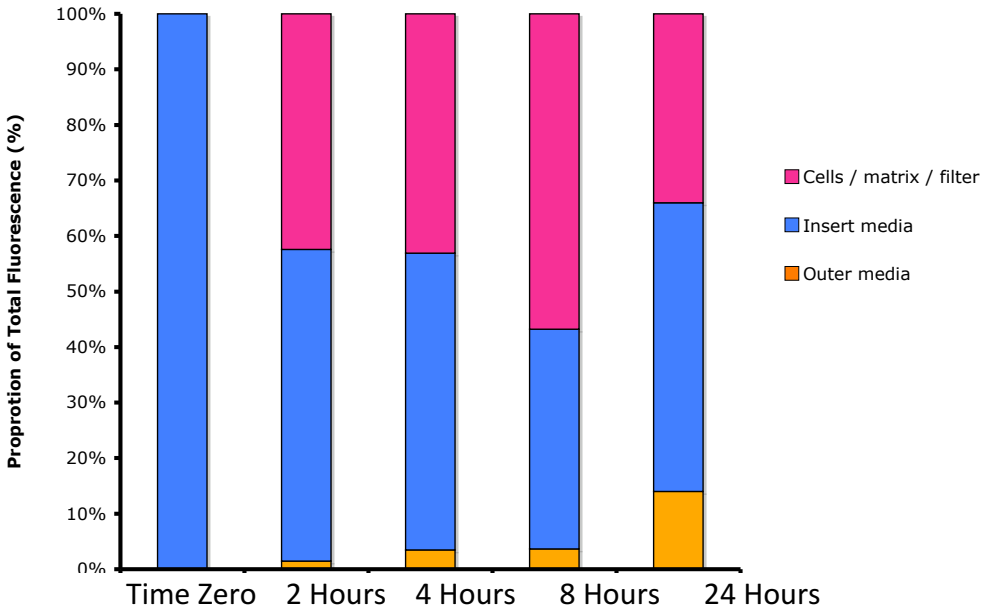


***Figure 6:*** *Analysis of the distribution of fluorescence in transwell filter cultures by fluorescence spectroscopy.*